Desalination and Water Treatment
www.deswater.com

doi: 10.5004/dwt.2021.26642

212 (2021) 276–285
February

Experimental investigation of the effect of ion concentration and its valence on reflection coefficient and solute permeability of NF membranes

Amal Al-Saadi[a], Hasan Mousa[a,b,*], G. Reza Vakili-Nezhaad[a,*], Ashish M. Gujarathi[a]

[a]*Department of Petroleum and Chemical Engineering, Sultan Qaboos University, P.C. 123, P.O. Box: 33, Muscat, Oman, email: hasana@squ.edu.om (H. Mousa)*
[b]*Department of Chemical Engineering, Jordan University of Science and Technology, P.O. Box: 3030, Irbid 22110, Jordan*

Received 9 April 2020; Accepted 30 September 2020

ABSTRACT

The objective of this manuscript is to investigate experimentally and theoretically the effect of ion (cation and anion) valence and concentration on the rejection coefficient and solute permeability of NF270 membrane. The experimental data of solute rejection vs. permeate flux is usually fitted to Spiegler–Kedem equation to determine the reflection coefficient and the solute permeability. In doing so, many problems may arise such as inaccurate numerical fitting, the discrepancy in the results when the different initial guess is made and sometimes no result is obtained. The current research work overcomes these problems by transferring the Spiegler–Kedem equation to a one-parameter equation. This is done by first using the flux equation to determine the rejection coefficient and use this data in the Spiegler–Kedem equation to determine the solute permeability. The success of this procedure was confirmed by comparing its results with those available in open literature where an excellent agreement was found. Moreover, the values of the reflection coefficient and the solute permeability that some researchers could not determine were found. The interaction between the solutes especially at high concentrations was taken into account when the osmotic pressure was calculated. The experimental results showed that σ is inversely proportional to the concentration. P_s, however, are proportional to the concentration until a certain concentration is reached after which the effect diminishes. The results also show that as the valence of the cation increases both σ and P_s increase. The results showed that $AlCl_3$ has the highest value of σ and NaCl has the lowest value. The values of σ follow the following order: $\sigma_{AlCl_3} > \sigma_{MgCl_2} > \sigma_{Na_2SO_4} > \sigma_{NaCl}$. The dependence of P_s on the solute type follows the following order $P_{s,NaCl} > P_{s,Na_2SO_4} > P_{s,MgCl_2} > P_{s,AlCl_3}$.

Keywords: Nanofiltration; Membrane; Reflection coefficient; Permeability; Rejection

1. Introduction

Nanofiltration (NF) technology is a pressure-driven membrane technology used for ion separation and treating wastewater due to its small pore size that lies ranges between 0.5 and 2 nm [1,2]. Nanofiltration processes have been used for over five decades to produce freshwater [3]. Manufacturers produce NF membranes of various specifications that make it suitable for specific separation processes. Moreover, the NF membrane has numerous preferable features such as high rejection of the single and multi-solutes systems, high flux, and low operating pressure [4]. Sea or brackish water pretreatment by NF membranes has been applied in water desalination by reverse osmosis (RO) processes, which solves many desalination issues like fouling and scaling [5]. The NF membrane has also been utilized directly to treat seawater [3]. NF is mostly operated under pressure ranges between 7 and 30 bars [6]. These types of membranes have a high flux compared to RO.

* Corresponding authors.

NF membranes are generally made from polymeric materials such as polysulfone, polyacrylonitrile, or inorganic materials such as ceramic. Polymeric membranes are usually used with drinking water and wastewater processes [7]. NF membranes involve a variety of separation phenomena such as diffusion, convection, and electromigration [8]. Different types of commercial NF membranes (NF270, NF90, and NF30) were used to treat seawater. Among all membranes, NF90 has a smaller pores size, high surface roughness, and high porosity. This membrane has the highest solute rejection while NF30 has the lowest solute rejection [9]. Some operational factors can influence the removal capacity of the NF membranes like a salt concentration in the feed, applied pressure, and pH [6].

Boussouga and Lhassani [10] and Ballet et al. [11] studied the mass transfer phenomena for some salts (NaCl, Na_2SO_4, and $MgSO_4$) using commercial NF membranes (NF90 and NF270). The studies showed that the rejection of SO_4^{-2} reaches 99% using NF90 while it reaches 96% with NF270. This was attributed to the smaller pore size of the NF90 membrane compared to that of NF270. The studies also showed that the rejection of monovalent salts such as Na^+ (47%) using NF270 is much lower than that of the divalent salts such as Mg^{2+} (96%). NF90 also showed higher retention compared to NF270 since NF90 has a smaller pore size [12].

Membrane technology is practically implemented and is extensively used in various processes. However, the solute transport phenomenon is still not fully understood in detail. NF separation is a very sophisticated process [13] and hence many models have been modified for membrane separation mechanism, which can be categorized into two main groups: irreversible thermodynamic models and transport mechanism models.

The performance of any type of membrane is described by the reflection coefficient (σ) the value of which ranges between 0 and 1 for NF membranes. The value of σ reflects the membrane's ability to catch the solute and prevents its passage [14]. Researchers have used the Spiegler–Kedem model intensively to determine salt permeability (P_s) and reflection coefficient (σ) [15–17]. These factors can be found using the best-fit method of the experimental data of rejection vs. permeate flux. Zouhri et al. [18] applied Spiegler–Kedem model using three NF membranes (NF270*4040, NF90*4040, and TR60) and two RO membranes (BW30LE4040 and TM710) to predict membrane performance and successfully determined σ and P_s.

Determining σ and P_s by fitting the measured permeate flux and solute rejection to Spiegler–Kedem equation may lead to inaccurate results since the values depend on the initial guess made. In some cases, it is not possible to determine them due to numerical instabilities and sometimes illogical values may result. The objective of this work suggests a method to overcome these problems by first determining σ using the solute flux equation and use the determined value of σ in Spiegler–Kedem equation which becomes a one parameter equation that enables determining the value of P_s. This work also aims at experimentally investigating the effect of the valence of the ions (both the cation and the anion) and their concentration on σ and P_s. The interaction between solutes when the concentration is high was taken into account when calculating the osmotic pressure a situation that was not dealt with previously.

2. Theory

Spiegler–Kedem model is derived from Kedem–Katchalsky theory where the solvent (J_v) and the solute (J_s) fluxes are represented by the following equations:

$$J_v = p_I\left[\frac{dp}{dx} - \sigma\frac{d\pi}{dx}\right] \tag{1}$$

$$J_s = P_s \cdot \Delta C + \left(1-\sigma\right)CJ_v \tag{2}$$

where p is the applied pressure, x is membrane thickness, C is solute concentration. Eqs. (1) and (2) indicate that the volumetric and the solute fluxes are controlled by the solute reflection coefficient, σ, and the solute permeability, P_s. Careful estimation of these parameters allows finding the fluxes. Kedem and Katchalsky [19] proposed a relationship between the volumetric flux (J_v) and the observed rejection coefficient (R_0) given by the following equation:

$$\frac{R_0}{1-R_0} = \frac{\sigma}{1-\sigma}\left[1-e^{\left(-\frac{1-\sigma}{P_s}\right)J_v}\right] \tag{3}$$

where R_0 is the observed rejection coefficient defined as:

$$R_0 = 1 - \frac{C_p}{C_f} \tag{4}$$

where C_p and C_f are the concentration of the solute in the permeate and in the feed, respectively.

Accordingly, the values of σ and P_s are determined by fitting the experimental data of $\frac{R_0}{1-R_0}$ and J_v to Eq. (3). The accuracy of the fitting depends on the initial estimate of the parameters and if inappropriate initial guess is made, a false result may be obtained or in some cases, no results might be obtained. Moreover, fitting the data to Eq. (3) may result in numerical instabilities and the solution is divergent. In some cases, a good fit is obtained but the results of σ and P_s do not make sense [20–22].

To overcome the above-mentioned problems we propose the following procedures to determine σ and P_s based on the transport equation that relates the flux to the applied transmembrane pressure, ΔP, given by [23]:

$$J_v = L_p\left(\Delta P - \sigma\Delta\pi\right) \tag{5}$$

where L_p is hydraulic permeability of the membrane and $\Delta\pi$ is the osmotic pressure. σ is the reflection coefficient expressed as $\sigma = \left(\frac{\Delta P}{\Delta\pi}\right)_{J_v=0}$ and it specifies the selectivity of the NF membrane and the ability of the ions and the solutes to transfer through the membrane. For ideal membranes, for example, RO membranes, the value of σ reaches 1 due to RO's small pore size [24–26]. On the contrary, σ approaches to value of zero for membranes in which concentration gradient doesn't exist and that is because the membrane pore size is large compared to the ion or solute size such as MF membranes [25]. For the NF membrane, the reflection coefficient has a value less than 1 because it has a relatively larger pore size compared to the size of the solutes [22,27].

Eq. (5) indicates that L_p and σ can be determined by plotting J_v vs. ΔP where the slope is equal to L_p and the intercept is equal to $L_p\sigma\Delta\pi$ from which the value of σ is estimated once the osmotic pressure is calculated.

The osmotic pressure $\Delta\pi$ is influenced by solute concentration. For a dilute solution, the $\Delta\pi$ can be estimated using the Van't Hoff equation:

$$\Delta\pi = aC \tag{6}$$

where:

$$a = \frac{R_g T}{m} \tag{7}$$

It should be mentioned that, this Eqs. (7) is not valid for high concentration solutions used in the NF system. Therefore, the osmotic pressure $\Delta\pi$ can be estimated from the following equations written as [28]:

$$\varnothing = 1 - \frac{A\left|Z_+ Z_-\right|}{B^2 T^{1/2} a^2} \cdot \left[\frac{2}{I^{1/2}} - \frac{1}{(Ba)^{-1} T^{1/2} + I^{1/2}} - \frac{2\ln\left(1 + BaT^{-1/2} I^{1/2}\right)}{BaT^{-1/2} \cdot I}\right] + \frac{S}{T} \cdot \frac{2n}{2n+1} \cdot \frac{I^{2n}}{v_+ + v_-} \tag{8}$$

where A = 6,064.613 kg$^{1/2}$ mol$^{-1/2}$ K$^{3/2}$ and B = 56.827 kg$^{1/2}$ mol$^{-1/2}$ K$^{1/2}$.

Parameters S, a, and n are given in [28] where S is solvation parameter of anion, a is ion–ion distance parameter, and n is the ion–solvent distance parameter with the assumption of $n > 0$.

For $AlCl_3$ Bromley [29] suggested the following equation to calculate $\Delta\pi$ for $AlCl_3$:

$$1 - \varnothing = 2.303 A_\gamma \left|Z_+ Z_-\right| \frac{I^{\frac{1}{2}}}{3} \sigma\left(\rho I^{\frac{1}{2}}\right) - 2.303\left(0.06 + 0.6B\right)\left|Z_+ Z_-\right| \frac{I}{2}\Psi\left(aI\right) - 2.303B\frac{1}{2} \tag{9}$$

Here, ρ = 1 and $a = 1.5/|Z_+Z_-|$.

$$\sigma\left(\rho I^{\frac{1}{2}}\right) = \frac{3}{\left(\rho I^{\frac{1}{2}}\right)^3}\left[1 + \rho I^{\frac{1}{2}} - \frac{1}{1 + \rho I^{\frac{1}{2}}} 2\ln\left(1 + \rho I^{\frac{1}{2}}\right)\right] \tag{10}$$

$$\Psi\left(aI\right) = \frac{2}{aI}\left[\frac{1 + 2aI}{\left(1 + aI\right)^2} - \frac{\ln\left(1 + aI\right)}{aI}\right] \tag{11}$$

The solute may pass through the membrane by either diffusion, which is due to concentration gradient across the membrane (no pressure is applied in this case), or by convection when pressure is applied across the membrane.

The proposed procedure is as follows: the value of σ is first determined from a plot of J_v vs. ΔP where the slope is equal to L_p and the intercept is equal to $L_p\sigma\Delta\pi$. The value of $\Delta\pi$ is calculated from Eqs. (8) or (9). Once σ is known its value is substituted in Eq. (3) which will have one parameter in this case and that is P_s. Fitting the data $\left(\frac{R_0}{1 - R_0} \text{ and } J_v\right)$ using Eq. (3) is now straight forward and quick conversion is obtained. By this way all, the fitting problems (initial guess effect, numerical instabilities, and inaccuracy of the results) are avoided. To check the adequacy of this procedure the obtained values of σ and P_s are compared to those obtained by other researchers. Moreover, the values of σ and P_s that were not determined by some researchers are estimated and reported.

Once σ and P_s are known the rejection can be estimated for any value of J_v from Spiegler–Kedem equation as given through Eqs. (12) and (13) [30]:

$$R = \frac{\sigma\left(1 - F\right)}{1 - \sigma F} \tag{12}$$

$$F = \exp^{\left[-\frac{(1-\sigma)}{P_s} J_v\right]} \tag{13}$$

$$P_s = \frac{-\left(1 - \sigma\right) J_v}{\ln F} \tag{14}$$

2.1. Procedure verification

To prove the accuracy and adequacy of the suggested procedure of estimating σ and P_s, the results obtained by other researcher and by the suggested procedure for NF270 membrane are tabulated in Table 1. The result presented in Table 1 shows that an excellent agreement between the values of σ and P_s exists. The results justify the easiness and the adequacy of the proposed procedure. It can also be seen from Table 1 that values that were not possible to determine by the two models fit and by the researchers are easily determined by the suggested procedure.

Al-Zoubi and Omar [22] estimated the parameters σ and P_s for some anions and cations (Na^+, Cl^-, SO_4^{2+}, and Mg^{2+}) using NF270 and NF90 membranes. A comparison between their reported results and those obtained using the proposed procedures is summarized in Table 2. Again, a good agreement is obtained between the results. It is clear from Table 2 that the rejection (and hence σ and P_s) is strongly affected by the type of cation or anion which in turns affects the estimated values of σ and P_s.

The adequacy of the proposed procedure to determine σ and P_s for NF30 type membrane is shown in Table 3 where its results are compared to those obtained by other researchers and by the two models fit of Eq. (3). A good agreement between the results is obtained. The results in Table 3 prove the adequacy of the proposed procedure especially for

Table 1
List of the values of σ and P_s obtained using Kedem and Katchalsky (Eq. (3)), the proposed procedures (Eq. (5)), and those listed in the literature for various types of salts and various concentrations for NF270 membrane

Membrane		NF270							Reference
Salts		C (ppm)	Proposed procedure		Two parameter numerical fit		Reported values		
			σ	P_s (L m^{-2} h)	σ	P_s (L m^{-2} h)	σ	P_s (L m^{-2} h)	
		5,000	0.98	91.17	1.07	86.88	0.95	75.1	
KCl		10,000	0.91	104.29	1.09	121.76	0.99	109	
		15,000	0.94	118.56	0.99	157.7	0.99	132	
		3,000	0.98	0.27	0.99	0.21	0.98	0.31	
Na_2SO_4		5,000	0.96	0.38	1.00	0.31	0.98	0.44	[21]
		10,000	0.99	0.47	0.88	0.43	0.99	0.90	
		5,000	0.95	3.61	1.08	1.36	0.98	0.54	
$MgSO_4$		10,000	0.98	4.13	0.96	1.65	0.97	0.68	
		15,000	0.98	7.89	0.83	0.85	0.97	1.04	
Mixture of	Na^+	11,460	0.63	152.99	*	177.78	*	168	
NaCl and	Cl^-	15,194	0.81	223.39	*	261.97	*	395	
$NaSO_4$	SO_4^{2-}	3,379	1.16	2.81	0.93	1.86	0.92	1.76	[22]
Mixture of	Na^+	11,008	0.89	138.49	0.94	189.35	*	160	
NaCl and	Cl^-	18,389	0.93	129.05	0.95	204.03	0.93	264	
$MgCl_2$	Mg^{2+}	479	0.70	10.83	0.81	7.43	*	9.6	

*values are not obtained/available.

Table 2
List of the obtained values of σ and P_s using Eqs. (3) and (5) and those listed in the literature for various types of salts and various concentrations for NF90 membrane

Membrane		NF90							Reference
Ions		C (ppm)	Proposed procedure		Two parameter numerical fit		Reported values		
			σ	P_s (L m^{-2} h)	σ	P_s (L m^{-2} h)	σ	P_s (L m^{-2} h)	
Mixture of	Na^+	11,460	0.81	4.48	0.84	2.79	0.68	2.16	
NaCl and	Cl^-	15,194	0.65	1.67	*	2.85	*	4.80	
$NaSO_4$	SO_4^{2-}	3,379	0.87	0.49	0.88	0.28	0.85	0.23	[22]
Mixture of	Na^+	11,008	0.85	4.79	0.89	7.42	0.67	4.82	
NaCl and	Cl^-	18,389	0.71	3.24	0.58	3.35	0.59	3.12	
$MgCl_2$	Mg^{2+}	479	1.06	0.32	0.75	0.69	0.73	0.55	

*values are not obtained/available.

low concentration solutes where using Eq. (3) to estimate σ and P_s did not succeed.

3. Experimental work

3.1. Set up

Batch experiments are performed on pilot scale nanofiltration membrane system, the experimental setup is shown in Fig. 1. The system consists of a feed tank of 10 L capacity, a high pressure pump, membrane cell, and cooling system. The feed solution temperature was maintained at 30°C ± 1°C and the flow rate was constant at 6 L min^{-1}. A rectangular cell – flat sheet membrane – is utilized to carry on the batch experiments. The membrane-housing unit is made of stainless steel with two parts tight together with high tensile screws. The upper half of membrane cell contained the flow distribution cavity and a groove to fix rubber ring to avoid leakage at high pressure range. The base half is used to fix the membrane flat sheet as well as membrane supporting to prevent rupture at high applied pressures. The supporting arrangements layers contain 1 mm of a perforated plastic sheet on which Whatman#42 filter paper is laid on top of which the NF membrane is placed.

Table 3
List of the obtained values of σ and P_s using Eqs. (3) and (5) and those listed in the literature for various types of salts and various concentrations for NF30 membrane

Membrane	NF30							Reference
Salts	C (ppm)	Proposed procedure		Two parameter numerical fit		Reported values		
		σ	P_s (L m^{-2} h)	σ	P_s (L m^{-2} h)	σ	P_s (L m^{-2} h)	
KCl	5,000	0.92	165.85	0.89	*	*	*	[21]
	10,000	0.99	211.51	0.99	643.51	*	*	
	15,000	0.97	196.65	0.95	186.84	*	*	
Na_2SO_4	3,000	0.83	10.25	0.73	15.87	0.69	14.72	
	5,000	0.56	7.36	0.58	11.82	0.56	11.30	
	10,000	0.85	28.16	0.71	30.19	0.61	29.55	
$MgSO_4$	5,000	0.98	7.92	0.54	7.92	0.53	7.78	
	10,000	0.76	6.72	0.55	7.71	0.52	7.15	
	15,000	0.59	6.17	0.54	8.55	0.52	8.23	

*values are not obtained/available.

The active layer of the membrane is exposed to the feed flow. The effective filtration area of the membrane is 35 cm^2. A schematic diagram of the filtration unit is shown in Fig. 1.

3.2. Materials and chemicals

In this study, a commercial polyamide NF 270 membrane was used (flat sheet film NF membrane is from Dow Filmtec™). The experiments were conducted with synthetic solutions comprised of inorganic salts: sodium chloride (NaCl, purity 99.5%), magnesium chloride ($MgCl_2$, purity 95.2), sodium sulfate (Na_2SO_4, purity 99%), and aluminum chloride ($AlCl_3$, purity 99.99%). These salts were used either as single salt solution to study the effect of ion valence and concentration on rejection or mixed salt solution. Chemicals were purchased from Sigma-Aldrich (Germany) and were used as received. The synthetic solutions were prepared with ultrapure water produced from the water

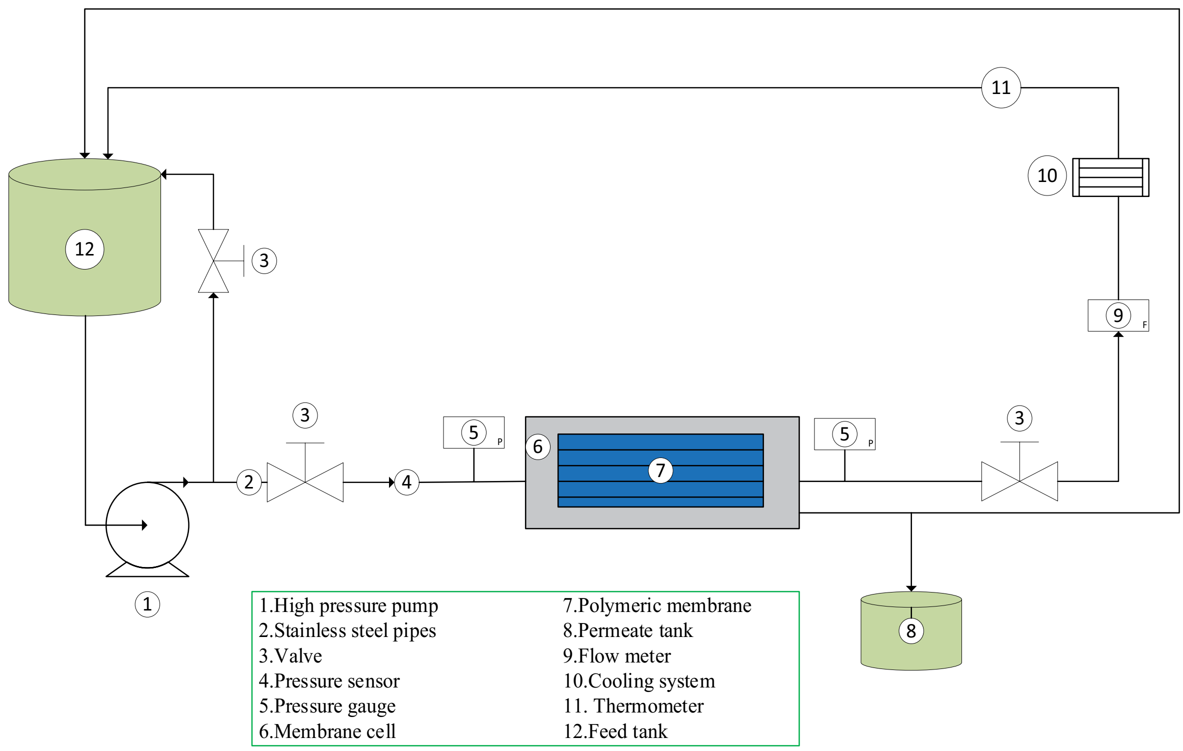

Fig. 1. Schematic of nano-filtration unit assembly.

purification unit (Milli-Q). The operating pressure was varied between 5 and 20 bar. The inlet feed concentration was varied in the range of 5,000–40,000 ppm. The concentrations of the salts for feed and permeate were analyzed using a conductivity meter (Mettler Toledo, seven Compact, USA).

4. Results and discussion

Experimental data on NF270, a commercial polyamide NF membrane collected from batch experiments to study the flux and rejection of sodium chloride (NaCl), sodium sulfate (Na_2SO_4), magnesium chloride ($MgCl_2$), and aluminum chloride ($AlCl_3$) are shown in Table 4. The values of σ and P_s were estimated by the procedures explained in the previous section. The values are also estimated by using the Spiegler–Kedem equation (Eq. (3)) to compare the results of the two methods. The results of the two methods are summarized in Table 4. The results showed an excellent agreement between the two methods.

4.1. Pure water permeability

The mean value of pure water permeability (solvent) L_p was measured before the salts rejection experiments by the statistical linear relationship of permeate flux vs. operating pressure. It was found to be 6.65×10^{-6} m s^{-1} bar. Later, this value of L_p will be considered as a reference to calculate reflection coefficient σ and solute permeability P_s. Fig. 2 shows pure water flux for NF270 membrane increase with the growth of operating pressure.

4.2. Effect of operating variables

4.2.1. Effect of concentration on NaCl, $MgCl_2$, $AlCl_3$, and Na_2SO_4 flux

Solute flux is affected by the concentration gradient across the two sides of the membrane and the solute mass transfer coefficient. Membranes material and construction also play an important role in solute permeation [31]. The experimental data of permeate flux of NaCl, $MgCl_2$, Na_2SO_4, and $AlCl_3$ vs. transmembrane pressure at different concentrations (5,000; 10,000; 20,000 and 40,000 ppm) are shown in Fig. 3. As can be seen from Fig. 3 a linear relation between the permeate flux and the applied pressure exists. It can also be seen that as the concentration increases the flux decreases. Data for the measured fluxes and rejection is shown in Table 4.

4.2.2. Effect of pressure on NaCl, $MgCl_2$, $AlCl_3$, and Na_2SO_4 rejection

In order to examine the impact of solute concentration on rejection, NaCl, $MgCl_2$, $AlCl_3$, and Na_2SO_4 concentrations were varied for 5,000; 10,000; 20,000 and 40,000 ppm at operating pressure range from 5 to 20 bar. The results are portrayed in Fig. 4 where it can be seen that salt rejection increases as the pressure increases for all solutes tested. It can be also seen that for a given value of *P*, the rejection increases as the concentration decreases. In addition, the rejection also decreased with increased feed concentration.

Table 4
Measured values of flux and solute retention for various salts at different concentrations and estimated values of σ and P_s using the proposed method and Eq. (3) for NF270 membrane at temperature of 30°C and feed flow rate of 6 L min^{-1}

Membrane	NF270						
Salt	C (ppm)	Flux (m s^{-1})	R_0	Proposed method		Two parameter numerical fit Eq. (3)	
				σ	P_s (m s^{-1})	σ	P_s (m s^{-1})
NaCl	5,000	5.98E-05	0.50	0.66	1.09E-05	0.69	1.07E-05
	10,000	5.37E-05	0.39	0.53	2.15E-05	0.57	2.20E-05
	20,000	4.78E-05	0.19	0.32	2.84E-05	0.31	2.94E-05
	40,000	4.34E-05	0.10	0.20	3.77E-05	*	*
$MgCl_2$	5,000	5.75E-05	0.52	0.53	7.91E-06	0.63	1.06E-05
	10,000	5.03E-05	0.43	0.46	1.22E-05	0.55	1.49E-05
	20,000	4.25E-05	0.34	0.38	1.51E-05	0.48	1.96E-05
	40,000	3.76E-05	0.20	0.23	1.69E-05	0.31	1.71E-05
$AlCl_3$	5,000	7.45E-05	0.58	0.74	5.46E-06	0.75	5.86E-06
	10,000	6.24E-05	0.53	0.69	9.53E-06	0.71	9.47E-06
	20,000	5.31E-05	0.47	0.64	1.28E-05	0.68	1.12E-05
	40,000	4.06E-05	0.34	0.36	1.54E-05	0.39	1.62E-05
Na_2SO_4	5,000	7.30E-05	0.52	0.58	9.88E-06	0.68	9.96E-06
	10,000	4.57E-05	0.37	0.53	1.71E-05	0.57	1.67E-05
	20,000	4.34E-05	0.23	0.47	2.22E-05	0.37	2.57E-05
	40,000	4.11E-05	0.13	0.25	2.54E-05	*	2.89E-05

*value were not obtained.

4.3. *Effect of concentration on σ*

The reflection coefficient (σ) of a given salt is the greatest possible rejection value for that solute. In this study, σ for NaCl, $MgCl_2$, Na_2SO_4, and $AlCl_3$ solutes is calculated

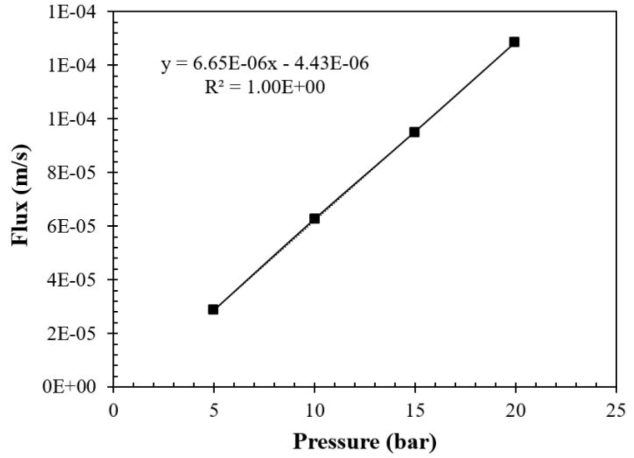

Fig. 2. Effect of applied pressure on pure water flux for NF270 membrane.

using the proposed procedure as mentioned in the theory section. The estimated values of σ for all the above salts are listed in Table 4. To illustrate the effect of concentration on σ, the calculated values of σ are plotted vs. concentration for all solutes tested and the results are shown in Fig. 5. It can be seen that σ is inversely proportional to the feed concentration. The results show that the data follows a linear fit ($\sigma = -a \times C + b$) with $a = 1 \times 10^{-6}$ for all salts tested and intercept varies according to the salt type. The R^2 values of all the fits are larger than 0.9. The results show that $AlCl_3$ has the highest values of σ whereas NaCl has the lowest values of σ. The dependence of σ on the type of solute follow the following order $\sigma_{AlCl_3} > \sigma_{MgCl_2} > \sigma_{Na_2SO_4} > \sigma_{NaCl}$.

4.4. *Effect of concentration on P_s*

Solute permeability, P_s, is influenced by three factors: salt concentration, nature of the solute, and the effective charge of the NF membrane [32]. Estimated values of P_s as a function of solute concentration are shown in Fig. 6. It can be seen that P_s increases as the concentration increases. Fig. 6 shows that the effect is larger until the concentration reaches a certain value then the effect becomes small. It can be also noticed as the solute size decreases (cation size) the value of P_s increases. Accordingly, NaCl has

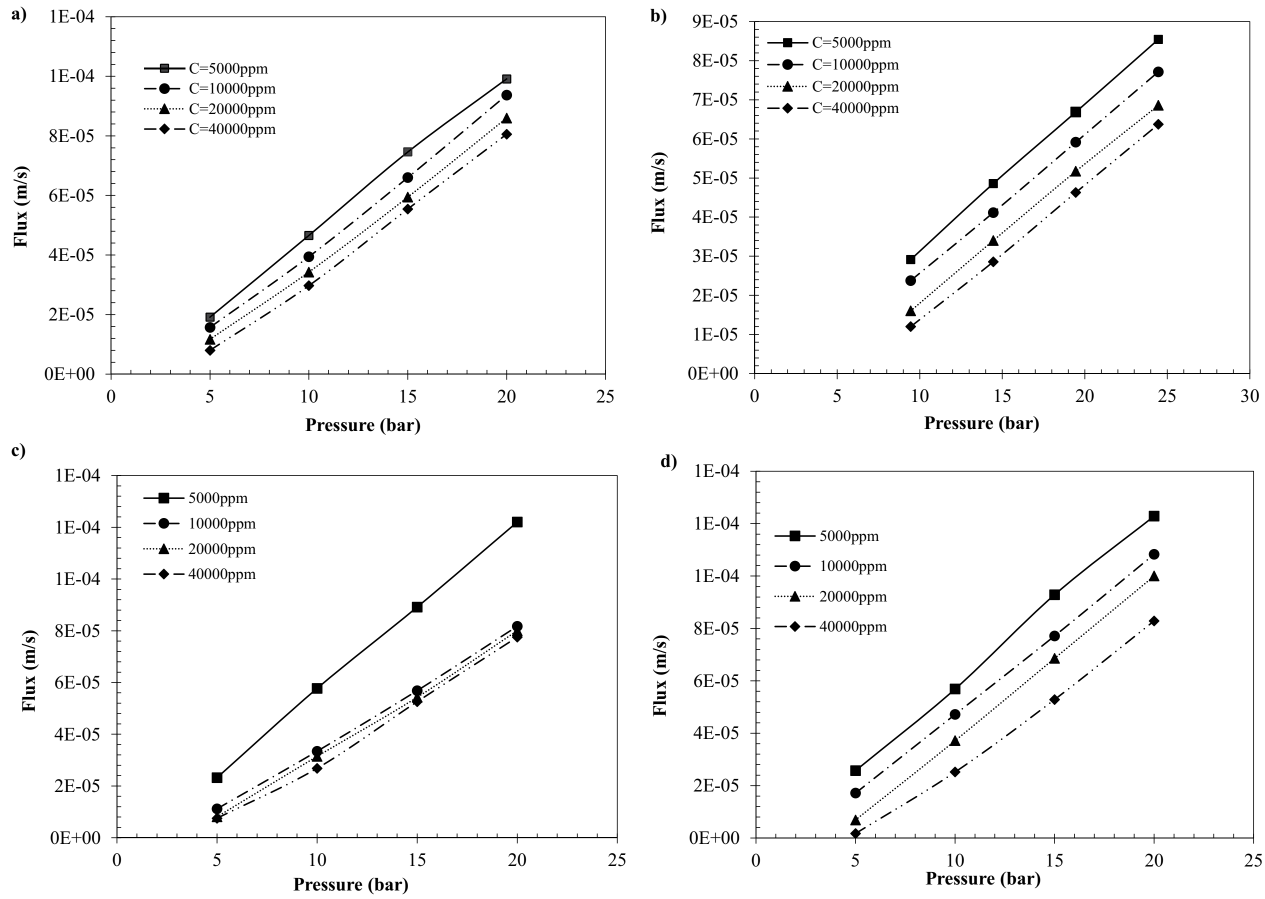

Fig. 3. Measured permeate flux vs. the applied pressure for various concentration (at 6 L min^{-1} and 30°C) (a) NaCl, (b) $MgCl_2$, (c) Na_2SO_4, and (d) $AlCl_3$.

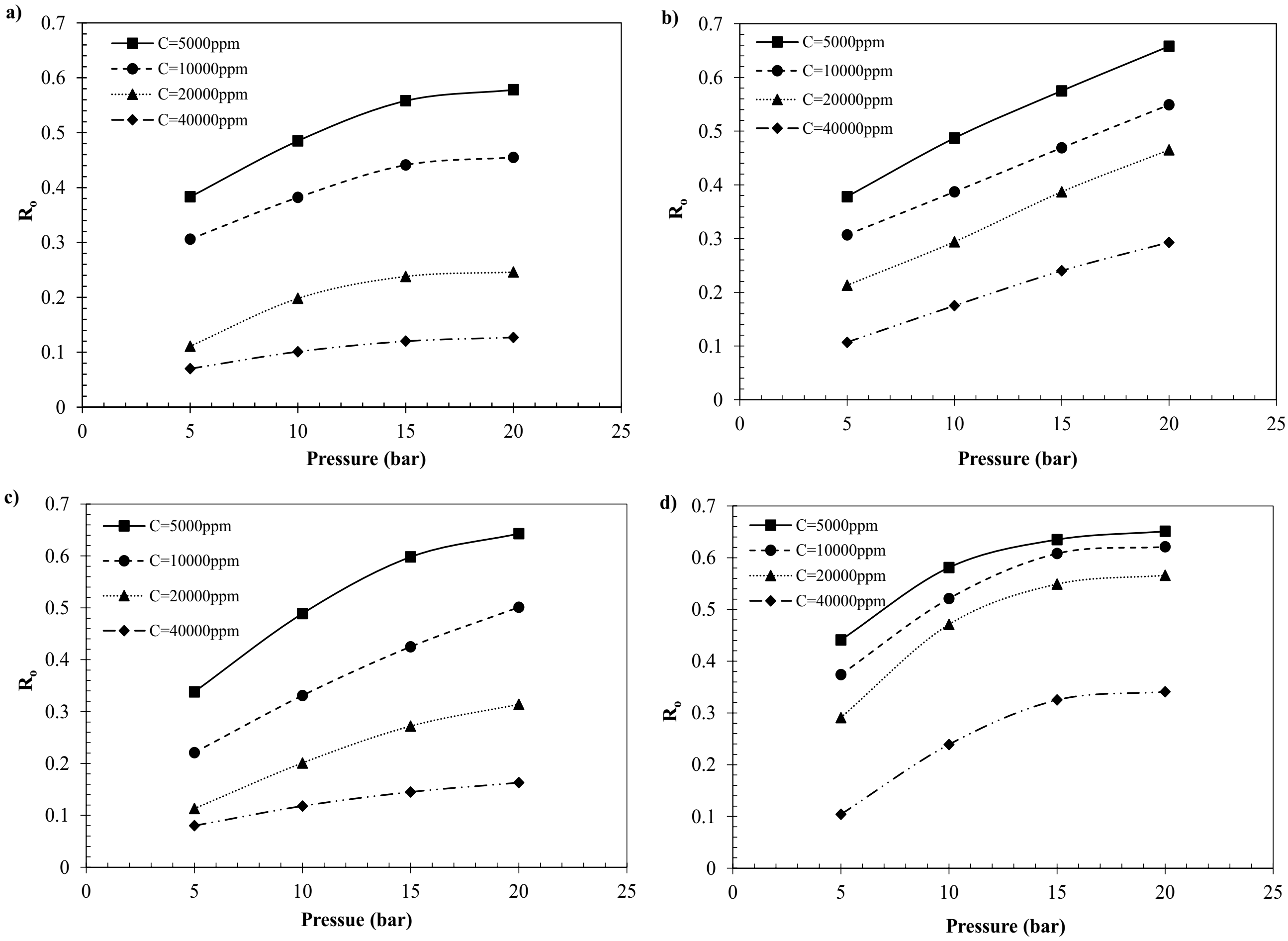

Fig. 4. Rejection as a function of the applied pressure for various concentration (at 6 L min^{-1} and 30°C) (a) NaCl, (b) $MgCl_2$, (c) Na_2SO_4, and (d) $AlCl_3$.

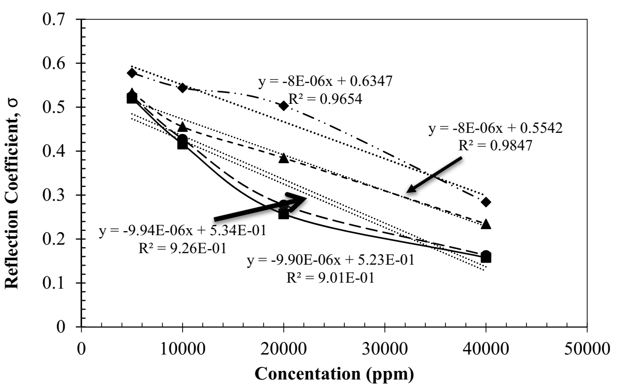

Fig. 5. Estimated reflection coefficient vs. concentration for the various ions tested. ◆ $AlCl_3$, ▲ $MgCl_2$, ● Na_2SO_4, and ■ NaCl. The lines represent the fitting of the data.

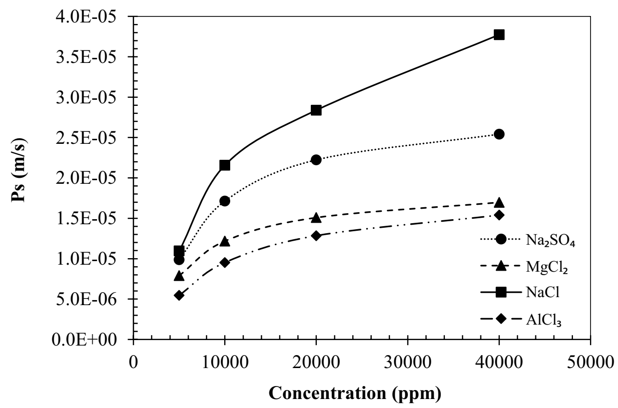

Fig. 6. Estimated values of P_s for the various solutes tested vs. concentration. ◆ $AlCl_3$, ▲ $MgCl_2$, ● Na_2SO_4, and ■ NaCl. The lines represent the fitting of the data.

the largest P_s value whereas $AlCl_3$ has the lowest P_s value. Moreover, when the anion size increases P_s value decreases and hence P_s value for NaCl is larger than that of Na_2SO_4. For other solutes, the dependence of P_s on the solute type follows the following order $P_{s,NaCl} > P_{s,Na_2SO_4} > P_{s,MgCl_2} > P_{s,AlCl_3}$.

5. Conclusion

The rejection of various solutes through the NF270 membrane was experimentally investigated. Membrane parameters (reflection coefficient, σ, and solute permeability,

P_s) were determined. All of the numerical problems that were previously encountered were overcome by using the flux equation then Spiegler–Kedem model. Solute interaction especially at high concentration was taken into account when calculating the osmotic pressure. The effect of solute concentration and its type on the membrane parameters was experimentally investigated. The results showed that as the concentration increases σ decreases linearly. However, the value of P_s increases as the concentration of the solute increases. The results also showed that P_s increases rapidly with concentration until a certain concentration is reached after which no effect of concentration on P_s was noticed. The type of solute affects both σ and P_s. For the solutes tested, $AlCl_3$ has the highest value of σ and NaCl has the lowest value. The values of σ follow the following order: $\sigma_{AlCl_3} > \sigma_{MgCl_2} > \sigma_{Na_2SO_4} > \sigma_{NaCl}$. The dependence of P_s on the solute type follows the following order $P_{s,NaCl} > P_{s,Na_2SO_4} > P_{s,MgCl_2} > P_{s,AlCl_3}$.

Acknowledgment

The authors appreciate the financial support of Sultan Qaboos University and University of South Africa through the joint research funding (CL/SQU-SA/18/04).

Nomenclature

ΔP	—	Transmembrane pressure, bar
$\Delta\pi$	—	Osmotic pressure, bar
$\lvert Z_+Z_-\rvert$	—	Absolute value of the charge product
A_γ	—	Debye–Huckel constant for activity coefficient. It is equal to 0.511 $Kg^{1/2}$ $mol^{-1/2}$ at 25°C
C	—	Solute concentration, ppm
I	—	Ionic strength
J_s	—	Solute flux, m s^{-1}
J_v	—	Volumetric flux, m s^{-1}
L_p	—	hydraulic permeability of the membrane, m s^{-1} bar
p_i	—	Intrinsic membrane permeability, m s^{-1} bar
P_s	—	Solute permeability coefficient, m s^{-1}
T	—	Temperature, °C
σ	—	Reflection coefficient
ϕ	—	Osmotic coefficient
$\psi(aI)$	—	Function of *aI* as written in Eq. (9)

References

[1] E. Coutinho de Paula, P.V. Martins, I.C.d.M. Ferreira, M.C.S. Amaral, Bench and pilot scale performance assessment of recycled membrane converted from old nanofiltration membranes, Environ. Technol., 41 (2020) 1232–1244.

[2] A. Ghorbani, B. Bayati, T. Kikhavani, Modelling ion transport in an amine solution through a nanofiltration membrane, Braz. J. Chem. Eng., 36 (2019) 1667–1677.

[3] D.L. Oatley-Radcliffe, M. Walters, T.J. Ainscough, P.M. Williams, A.W. Mohammad, N. Hilal, Nanofiltration membranes and processes: a review of research trends over the past decade, J. Water Process Eng., 19 (2017) 164–171.

[4] A. Pérez-González, R. Ibáñez, P. Gómez, A.M. Urtiaga, I. Ortiz, J.A. Irabien, Nanofiltration separation of polyvalent and monovalent anions in desalination brines, J. Membr. Sci., 473 (2015) 16–27.

[5] J. Kavitha, M. Rajalakshmi, A. Phani, M. Padaki, Pretreatment processes for seawater reverse osmosis desalination systems— a review, J. Water Process Eng., 32 (2019) 100926–100938, doi: 10.1016/j.jwpe.2019.100926.

[6] A.M. Hidalgo, G. León, M. Gómez, M.D. Murcia, E. Gómez, J.L. Gómez, Application of the Spiegler–Kedem–Kachalsky model to the removal of 4-chlorophenol by different nanofiltration membranes, Desalination, 315 (2013) 70–75.

[7] F.N. Ahmed, Modified Spiegler–Kedem Model to Predict the Rejection and Flux of Nanofiltration Processes at High NaCl Concentrations, Ph.D. Thesis, University of Ottawa, 2013.

[8] M.M. Zerafat, M. Shariati-Niassar, S.J. Hashemi, S. Sabbaghi, A.F. Ismail, T. Matsuura, Mathematical modeling of nanofiltration for concentrated electrolyte solutions, Desalination, 320 (2013) 17–23.

[9] N. Hilal, H. Al-Zoubi, A.W. Mohammad, N.A. Darwish, Nanofiltration of highly concentrated salt solutions up to seawater salinity, Desalination, 184 (2005) 315–326.

[10] Y.A. Boussouga, A. Lhassani, Performances of nanofiltration and low pressure reverse osmosis membranes for desalination: characterization and modelling, IOP Conf. Ser.: Mater. Sci. Eng., 186 (2017) 1128–1138, doi: 10.1088/1757-899X/186/1/012039.

[11] G.T. Ballet, L. Gzara, A. Hafiane, M. Dhahbi, Transport coefficients and cadmium salt rejection in nanofiltration membrane, Desalination, 167 (2004) 369–376.

[12] S. Mondal, C.-l. Hsiao, S. Ranil Wickramasinghe, Nanofiltration/reverse osmosis for treatment of coproduced waters, Environ. Prog., 27 (2008) 173–179.

[13] A. Kowalik-Klimczak, M. Zalewski, P. Gierycz, Prediction of the chromium(III) separation from acidic salt solutions on nanfiltration membranes using Donnan and steric partitioning pore (DSP) model, Archit. Civ. Eng. Environ., 3 (2016) 135–140.

[14] A.L. Ahmad, L.S. Tan, S.R.A. Shukor, Modeling of the retention of atrazine and dimethoate with nanofiltration, Chem. Eng. J., 147 (2009) 280–286.

[15] H. Kelewou, A. Lhassani, M. Merzouki, P. Drogui, B. Sellamuthu, Salts retention by nanofiltration membranes: physicochemical and hydrodynamic approaches and modeling, Desalination, 277 (2011) 106–112.

[16] H. Cao, M. O'Rourke, O. Habimana, E. Casey, Analysis of surrogate bacterial cell transport to nanofiltration membranes: effect of salt concentration and hydrodynamics, Sep. Purif. Technol., 207 (2018) 498–505.

[17] Z.V.P. Murthy, L.B. Chaudhari, Rejection behavior of nickel ions from synthetic wastewater containing Na_2SO_4, $NiSO_4$, $MgCl_2$ and $CaCl_2$ salts by nanofiltration and characterization of the membrane, Desalination, 247 (2009) 610–622.

[18] N. Zouhri, M. Igouzal, M. Larif, M. Hafsi, M. Taky, A. Elmidaoui, Prediction of salt rejection by nanofiltration and reverse osmosis membranes using Spiegler–Kedem model and an optimisation procedure, Desal. Water Treat., 120 (2018) 41–50.

[19] M. Bchiti, M. Igouzal, F. El Azhar, H. Oudda, A. El Midaoui, Modeling the separation performance of nanofiltration and reverse osmosis: case study of groundwater desalination (M'Nasra zone Morocco), Bulg. Chem. Commun., 51 (2019) 625–631.

[20] N. Hilal, H. Al-Zoubi, N.A. Darwish, A.W. Mohammad, Performance of nanofiltration membranes in the treatment of synthetic and real seawater, Sep. Sci. Technol., 42 (2007) 493–515.

[21] H. Al-Zoubi, N. Hilal, N.A. Darwish, A.W. Mohammad, Rejection and modelling of sulphate and potassium salts by nanofiltration membranes: neural network and Spiegler–Kedem model, Desalination, 206 (2007) 42–60.

[22] H. Al-Zoubi, W. Omar, Rejection of salt mixtures from high saline by nanofiltration membranes, Korean J. Chem. Eng., 26 (2009) 799–805.

[23] J. Kheriji, B. Hamrouni, Boron removal from brackish water by reverse osmosis and nanofiltration membranes: application of Spiegler–Kedem model and optimization, Water Supply, 16 (2015) 684–694.

[24] T.Y. Khalaf, Estimation of concentration polarization using the combined film theory/Spiegler–Kedem model and empirical correlation, Alnahrain J. Eng. Sci., 11 (2008) 322–328.

[25] M. Pontié, H. Dach, J. Leparc, M. Hafsi, A. Lhassani, Novel approach combining physico-chemical characterizations and

mass transfer modelling of nanofiltration and low pressure reverse osmosis membranes for brackish water desalination intensification, Desalination, 221 (2008) 174–191.
[26] L. Pino, C. Vargas, A. Schwarz, R. Borquez, Influence of operating conditions on the removal of metals and sulfate from copper acid mine drainage by nanofiltration, Chem. Eng. J., 345 (2018) 114–125.
[27] F. Wu, L. Feng, L. Zhang, Rejection prediction of isopropylantipyrine and antipyrine by nanofiltration membranes based on the Spiegler–Kedem–Katchalsky model, Desalination, 362 (2015) 11–17.
[28] X. Ge, X. Wang, M. Zhang, S. Seetharaman, A new three-particle-interaction model to predict the thermodynamic properties of different electrolytes, J. Chem. Thermodyn., 39 (2007) 602–612.
[29] L.A. Bromley, Thermodynamic properties of strong electrolytes in aqueous solutions, AIChE J., 19 (1973) 313–320.
[30] R.B. Merlet, C.R. Tanardi, I.F. Vankelecom, A. Nijmeijer, L. Winnubst, Interpreting rejection in SRNF across grafted ceramic membranes through the Spiegler–Kedem model, J. Membr. Sci., 525 (2017) 359–367.
[31] AWWA, Reverse Osmosis and Nanofiltration (M46): AWWA Manual of Practice (AWWA Manuals), 2nd ed., M. Valentine, Ed., American Water Works Association, Denver, USA, 2007.
[32] X. Wei, X. Bao, J. Wu, C. Li, Y. Shi, J. Chen, B. Lv, B. Zhu, Typical pharmaceutical molecule removal behavior from water by positively and negatively charged composite hollow fiber nanofiltration membranes, RSC Adv., 8 (2018) 10396–10408.